

# Supplementary Material: Provable Preconditioned Plug-and-Play Approach for Compressed Sensing MRI Reconstruction

Tao Hong, *Member, IEEE*, Xiaojian Xu, *Member, IEEE*, Jason Hu, *Student Member, IEEE*, and Jeffrey A. Fessler, *Fellow, IEEE*

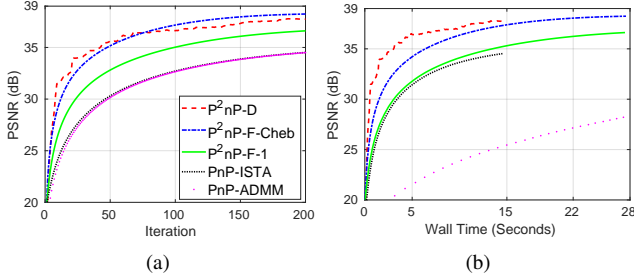


Fig. S.1. PSNR values versus iteration and wall (GPU) time for the knee 1 test image with spiral acquisition.

## S.I. SPIRAL ACQUISITION RECONSTRUCTION

Figure S.1 presents the PSNR values versus iteration and wall time for the knee 1 image with spiral acquisition. Clearly, we saw P<sup>2</sup>nP-F-1/Cheb and P<sup>2</sup>nP-D converged faster than PnP-ISTA and PnP-ADMM in terms of iteration number and wall time. Moreover, we observed P<sup>2</sup>nP-D was faster than P<sup>2</sup>nP-F-Cheb in terms of wall time, but P<sup>2</sup>nP-F-Cheb achieved higher PSNR eventually. In this setting, P<sup>2</sup>nP-F-1 was only slightly faster than PnP-ISTA and PnP-ADMM in terms of wall time. Figure S.2 shows the reconstructed images of each method. Obviously, P<sup>2</sup>nP required less iterations to achieve higher PSNR than PnP-ISTA and PnP-ADMM, illustrating the effectiveness of using preconditioners. Table S.I describes the results of other knee test images. Evidently, similar trend was observed for the brain test images.

## S.II. RADIAL ACQUISITION RECONSTRUCTION

Figure S.3 describes the PSNR values versus iteration and wall time of the brain 1 test image with radial acquisition. From Figure S.3, we observed P<sup>2</sup>nP converged faster than PnP-ISTA and PnP-ADMM. Moreover, P<sup>2</sup>nP-D converged similar to P<sup>2</sup>nP-F-Cheb in terms of iteration but P<sup>2</sup>nP-D was faster than P<sup>2</sup>nP-F-Cheb in terms of wall time. Table S.II shows the results of other test images, illustrating the effectiveness of adding preconditioners.

T. Hong is with the Department of Radiology, University of Michigan, Ann Arbor, MI 48109, USA (Email: tahong@umich.edu). TH was partly supported by National Institutes of Health grant R01NS112233.

J. Hu, X. Xu and J. Fessler are with the Department of Electrical and Computer Engineering, University of Michigan, Ann Arbor, MI 48109, USA (Email: {jashu, xjxu, fessler}@umich.edu).

## S.III. RADIAL ACQUISITION RECONSTRUCTION WITH 55 SPOKES

Figure S.5 describes the reconstruction of knee 1 test image with the 55 spokes radial acquisition. Clearly, the undesired artifacts in the 21 spokes radial acquisition disappeared and P<sup>2</sup>nP-D yielded the highest PSNR at 200th iteration.

## S.IV. CARTESIAN ACQUISITION RECONSTRUCTION

In this section, we present the results of using Cartesian sampling. Figure S.6 describes the downsampling mask and compares the PSNR values of different methods with respect to iteration and wall time for the knee 1 image. Moreover, we also tested the brain 1 image and the results are presented in Figure S.7. From Figures S.6 and S.7, we saw P<sup>2</sup>nP still outperforms than PnP-ISTA demonstrating the effectiveness of our approach.

## S.V. THE ACCELERATION FACTOR IN NON-CARTESIAN SAMPLING

In this section, we describe the method we used to compute the acceleration factor in non-Cartesian sampling. Without any confusion, the notation used in this section is self-contained.

For radial acquisition, the following formula is used to compute the acceleration factor (AF):

$$AF = \frac{N_{\text{spokes,fully sampled}}}{N_{\text{spokes,acquired}}}.$$

We approximate  $N_{\text{spokes,fully sampled}}$  through the number of phase encoding lines in Cartesian sampling.

For spiral acquisition, the number of interleaves required for full k-space coverage should ensure the spacing between adjacent spiral arms meeting the Nyquist criterion that

$$N_{\text{interleaves}} = \frac{2\pi k_{\text{max}}}{\Delta k},$$

where  $k_{\text{max}} = \frac{1}{2\Delta x}$  with  $\Delta x$  representing the image resolution and  $\Delta k \leq \frac{1}{\text{FOV}}$ . Then we have

$$N_{\text{interleaves}} = \frac{\pi \times \text{FOV}}{\Delta x} = \pi \times \text{Matrix Size}$$

resulting in

$$AF = \frac{N_{\text{interleaves}}}{N_{\text{acquired,interleaves}}}.$$

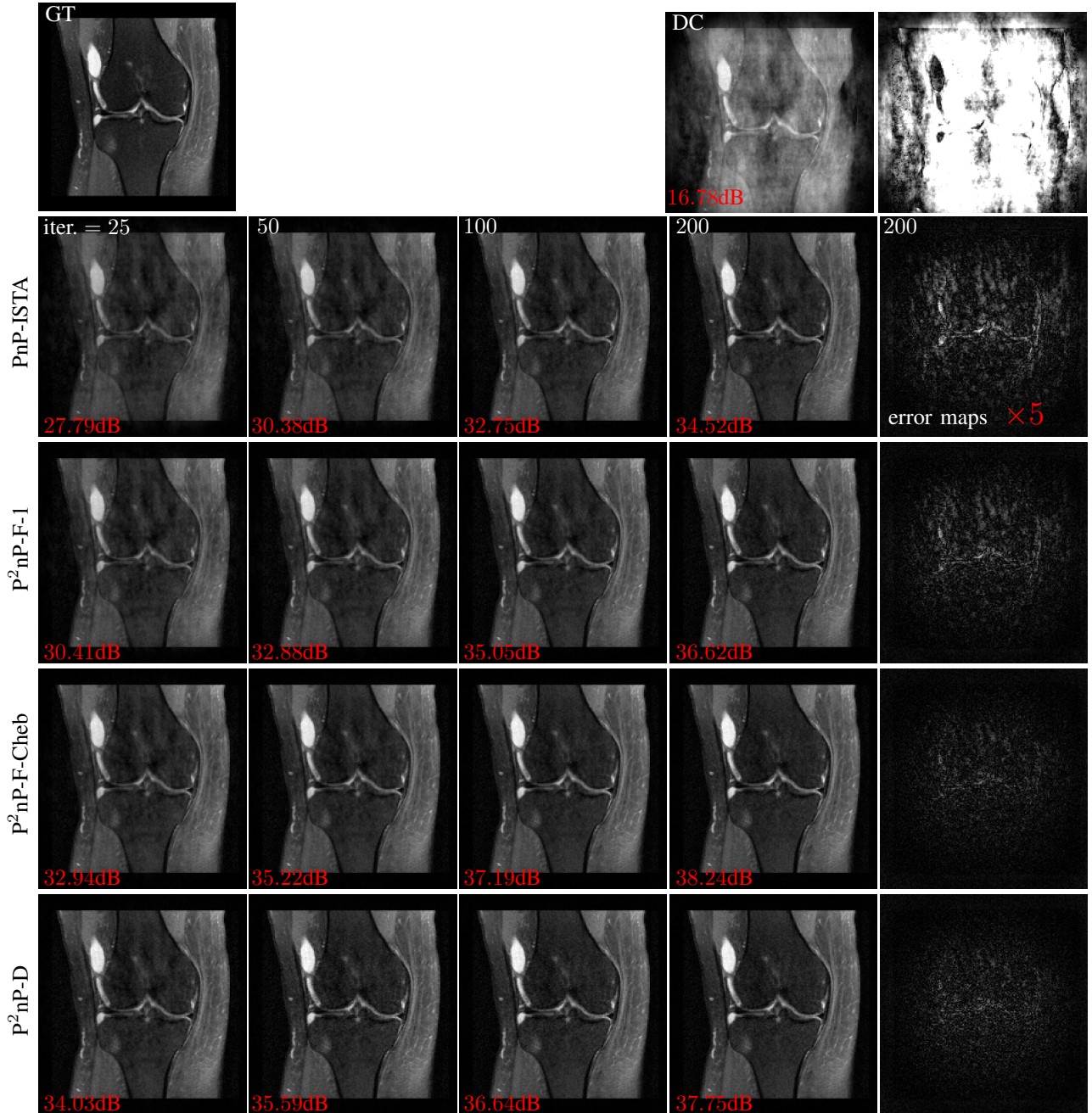


Fig. S.2. The reconstructed knee 1 images at 25, 50, 100, 200th iteration with spiral acquisition. The PSNR value is labeled in the left bottom corner of each image. The fifth column shown the error maps ( $\times 5$ ) of the reconstructed images at 200th iteration. We omitted the PnP-ADMM results since it is similar to PnP-ISTA. DC represents the density compensation based reconstruction. Acceleration factor is  $\approx 130$ .

TABLE S.I

PSNR PERFORMANCE OF EACH METHOD FOR RECONSTRUCTING 5 OTHER BRAIN TEST IMAGES WITH SPIRAL ACQUISITION. FOR PnP-ADMM, WE SHOWED THE MAXIMAL PSNR AND THE ASSOCIATED NUMBER OF ITERATIONS, AND WALL TIME THAT IS USED AS THE BENCHMARK. FOR OTHER METHODS ON EACH TEST IMAGE, THE SECOND COLUMN OF THE FIRST ROW REPRESENTS THE FIRST ITERATION THAT EXCEEDED PnP-ADMM PSNR. THE RELATED FIRST AND THIRD COLUMNS ARE THE ASSOCIATED PSNR AND WALL TIME, RESPECTIVELY. THE **BOLD** DIGITS DENOTE THE NUMBER OF ITERATIONS AND WALL TIME OF THE FASTEST ALGORITHM THAT FIRST EXCEEDED PnP-ADMM. THE SECOND ROW SHOWS THE PSNR AND WALL TIME AT THE 200TH ITERATION. THE **BLUE** DIGITS DENOTE THE HIGHEST PSNR AT THE 200TH ITERATION.

Index Methods	2			3			4			5			6		
	PSNR $\uparrow$	iter. $\downarrow$	sec. $\downarrow$	PSNR $\uparrow$	iter. $\downarrow$	sec. $\downarrow$	PSNR $\uparrow$	iter. $\downarrow$	sec. $\downarrow$	PSNR $\uparrow$	iter. $\downarrow$	sec. $\downarrow$	PSNR $\uparrow$	iter. $\downarrow$	sec. $\downarrow$
PnP-ADMM	37.85	200	147.8	34.33	200	148	34.96	200	147.4	33.53	200	148.9	34.24	200	147.8
PnP-ISTA	37.85	200	14.6	34.33	199	14.6	34.96	199	14.5	33.54	199	14.4	34.25	199	14.5
	37.85	200	14.6	34.34	200	14.7	34.97	200	14.6	33.55	200	14.5	34.26	200	14.6
P <sup>2</sup> nP-F-1	37.85	75	10.3	34.36	85	11.7	34.96	84	11.5	33.57	87	11.8	34.27	90	12.3
	39.03	200	27.4	36.43	200	27.5	36.73	200	27.5	35.92	200	27.2	36.44	200	27.4
P <sup>2</sup> nP-F-Cheb	37.91	37	5	34.36	41	5.7	34.99	41	5.6	33.56	42	5.7	34.28	44	6.1
	39.66	200	27.5	38.03	200	27.5	<b>38.15</b>	200	27.5	37.77	200	27.4	38.14	200	27.5
P <sup>2</sup> nP-D	38.34	<b>36</b>	<b>2.6</b>	34.33	<b>21</b>	<b>1.5</b>	35.06	<b>26</b>	<b>1.9</b>	33.58	<b>35</b>	<b>2.6</b>	34.29	<b>23</b>	<b>1.7</b>
	<b>39.80</b>	200	14.6	<b>38.23</b>	200	14.5	37.90	200	14.8	<b>38.04</b>	200	14.6	<b>38.21</b>	200	14.6

TABLE S.II

PERFORMANCE OF EACH METHOD ON THE RECONSTRUCTION OF OTHER BRAIN TEST IMAGES WITH RADIAL ACQUISITION. THE DEFINITION OF DIGITS IS IDENTICAL TO TABLE S.I. “—” MEANS THE METHOD CANNOT REACH HIGHER PSNR IN 200 ITERATIONS.

Index Methods	2			3			4			5			6		
	PSNR $\uparrow$	iter. $\downarrow$	sec. $\downarrow$	PSNR $\uparrow$	iter. $\downarrow$	sec. $\downarrow$	PSNR $\uparrow$	iter. $\downarrow$	sec. $\downarrow$	PSNR $\uparrow$	iter. $\downarrow$	sec. $\downarrow$	PSNR $\uparrow$	iter. $\downarrow$	sec. $\downarrow$
PnP-ADMM	30.76	181	134.5	31.31	181	132.7	30.79	182	133.3	29.63	175	129.1	29.23	163	121.8
PnP-ISTA	—	—	—	—	—	—	—	—	—	—	—	—	—	—	—
	30.73	200	14.5	31.29	200	14.3	30.77	200	14.4	29.59	200	14.4	29.14	200	14.4
P <sup>2</sup> nP-F-1	30.77	66	9.0	31.31	64	8.7	30.81	65	8.8	29.64	61	8.4	29.24	58	8.0
	31.38	200	27.4	31.95	200	27.3	31.46	200	27.2	30.25	200	27.3	29.67	200	27.5
P <sup>2</sup> nP-F-Cheb	30.80	33	4.6	31.35	32	4.4	30.83	32	4.3	29.66	30	4.1	29.23	28	3.8
	31.93	200	27.7	32.50	200	27.3	32.03	200	27.1	30.82	200	27.2	30.13	200	27.3
P <sup>2</sup> nP-D	30.77	<b>18</b>	<b>1.3</b>	31.41	<b>24</b>	<b>1.8</b>	30.83	<b>20</b>	<b>1.4</b>	29.66	<b>25</b>	<b>1.8</b>	<b>29.23</b>	<b>27</b>	<b>2.0</b>
	<b>32.07</b>	200	14.7	<b>32.68</b>	200	14.3	<b>32.04</b>	200	14.4	<b>30.51</b>	200	14.5	28.70	200	14.5

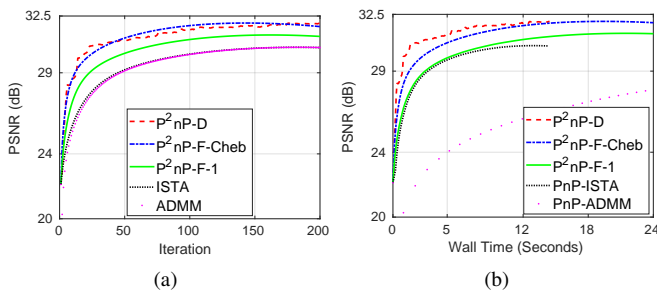


Fig. S.3. PSNR values versus iteration and wall (GPU) time for the brain 1 test image with radial acquisition.

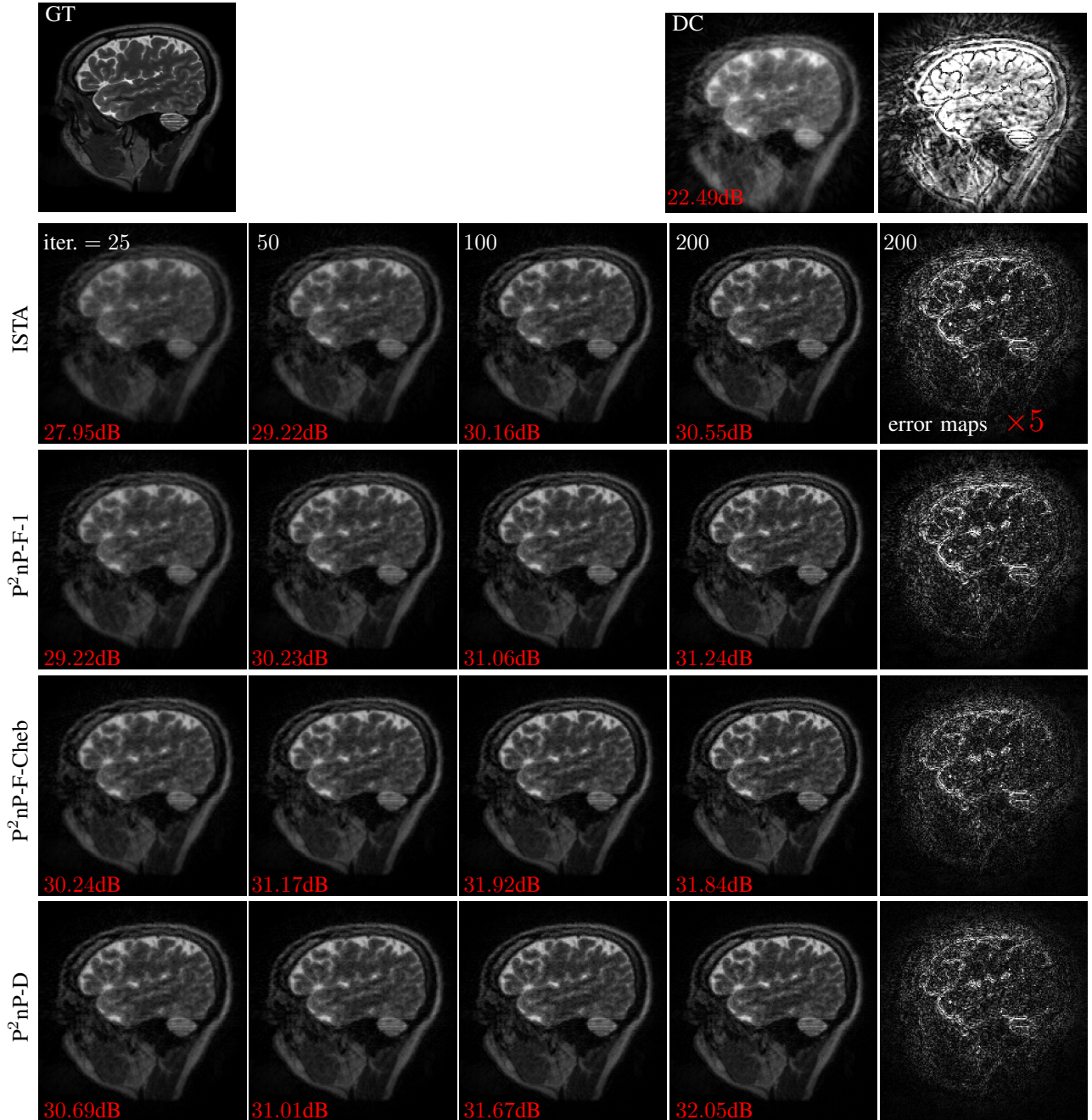


Fig. S.4. The reconstructed brain 1 images at 25, 50, 100, 200th iteration with different algorithms for radial acquisition. The PSNR value is labeled in the left bottom corner of each image. The fifth column shown the error maps ( $\times 5$ ) of the reconstructed images at 200th iteration. DC represents the density compensation based reconstruction. Acceleration factor is  $\approx 12$ .

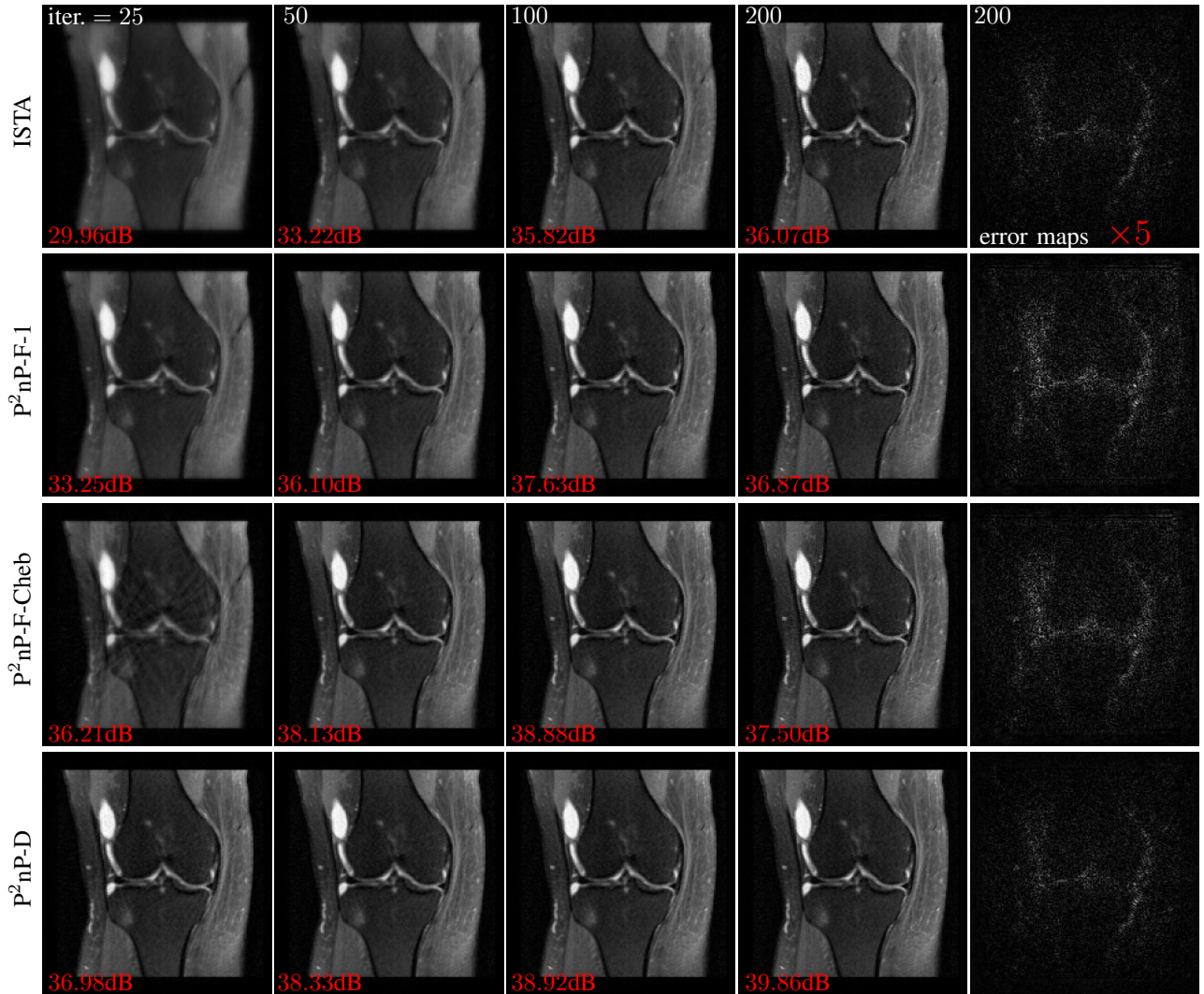


Fig. S.5. The reconstructed knee 1 images at 25, 50, 100, 200th iteration with radial acquisition of 55 spokes. The fifth column shown the error maps ( $\times 5$ ) of the reconstructed images at 200th iteration.

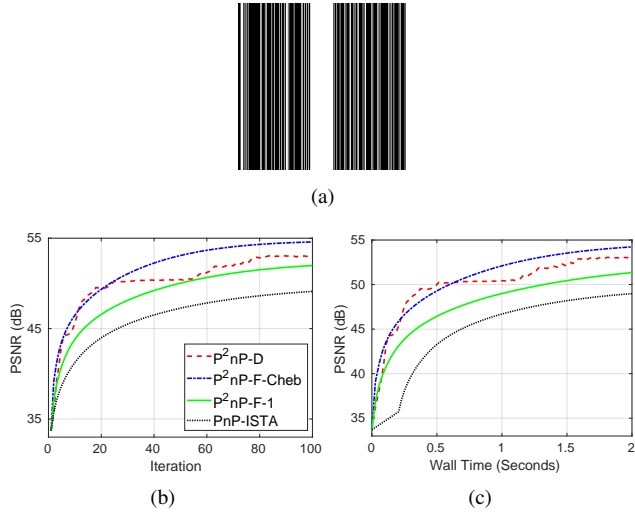


Fig. S.6. Downsampling mask and PSNR values versus iteration and wall time for the knee 1 image with Cartesian sampling. Acceleration factor is 2.

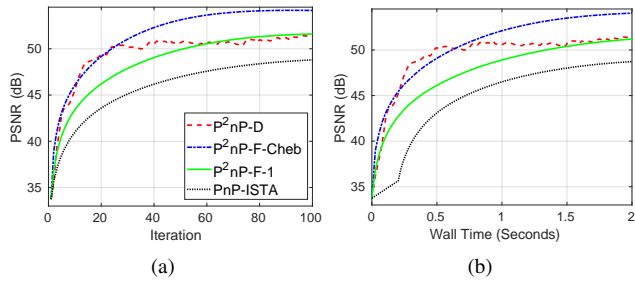


Fig. S.7. PSNR values versus iteration and wall time for the brain 1 image with Cartesian sampling.